WARSAW UNIVERSITY OF TECHNOLOGY Index 351733
FACULTY OF CIVIL ENGINEERING
COMMITTEE FOR CIVIL AND WATER ENGINEERING
POLISH ACADEMY OF SCIENCES ISSN 1230-2945

DOI: 10.24425/ace.2023.145277

ARCHIVES OF CIVIL ENGINEERING

Vol. LXIX ISSUE 2 2023

pp. 435 –453

Research paper

Analytical study on dynamic response of cantilever flexible retaining wall

Xiuzhu Yang[1], Xinyuan Liu[2], Shuang Zhao[3], Jun Yu[4]

Abstract: Based on wave mechanics theory, the dynamic response characteristics of cantilever flexible wall in two-dimensional site are analyzed. The partial derivative of the vibration equation of soil layer is obtained, and the general solution of the volume strain is obtained by the separation of variables method. The obtained solution is substituted back to the soil layer vibration equation to obtain the displacement vibration general solution. Combined with the soil-wall boundary condition and the orthogonality of the trigonometric function, the definite solution of the vibration equation is obtained. The correctness of the solution is verified by comparing the obtained solution with the existing simplified solution and the solution of rigid retaining wall, and the applicable conditions of each simplified solution are pointed out. Through parameter analysis, it is shown that when the excitation frequency is low, the earth pressure on the wall is greatly affected by the soil near the wall. When the excitation frequency is high, the influence of the far-field soil on the earth pressure of the wall gradually increases. The relative stiffness of the wall, the excitation frequency and the soil layer damping factor have a significant effect on the dynamic response of the flexible retaining wall.

Keywords: seismic analysis, flexible retaining wall, wave mechanics theory, dynamic response, analytic solution

[1]Prof., PhD., Central South University, School of Civil Engineering, Changsha, 410075, China, e-mail: xzyang1661@126.com, ORCID: 0000-0003-2316-2910

[2]MSc., Central South University, School of Civil Engineering, Changsha, 410075, China, e-mail: lxy2021@csu.edu.cn, ORCID: 0000-0001-8989-9531

[3]MSc., Central South University, School of Civil Engineering, Changsha, 410075, China, e-mail: zhaoshuang@csu.edu.cn, ORCID: 0000-0002-8761-0148

[4]Prof., PhD., Central South University, School of Civil Engineering, Changsha, 410075, China, e-mail: yujun@csu.edu.cn, ORCID: 0000-0002-5745-8157

1. Introduction

The dynamic response analysis of retaining wall is the basis of its seismic design. According to the wall stiffness, retaining wall is mainly divided into rigid wall and flexible wall. Under the action of earthquake, the rigid wall mainly depends on its own material strength and embedded depth of foundation to resist the impact of earthquake on the wall [1], and the flexible wall can rely on its deformation energy consumption to reduce the impact of earthquake on the wall [2]. In recent years, many scholars have put forward some practical simplified analysis methods for retaining wall design [3–5], such as response displacement method [6, 7], response acceleration method [8], static elastoplastic analysis method [9] and numerical simulation analysis method [10]. These methods have been widely used in engineering practice.

The wave method is a practical method to study the dynamic response of structures under earthquake. Based on the theory of wave mechanics, the dynamic response characteristics of structures are obtained by studying the propagation characteristics of vibration waves. Veletsos et al. [11, 12] established two two-dimensional semi-infinite site models of soil-flexible wall bonded on rigid bedrock. One model has elastic rotation constraint at the bottom of the wall, and the other model has the bottom of the wall rigidly connected to the rigid bedrock. Both models assume that there is no vertical stress in the soil medium. On this basis, the analytical solution of the dynamic response of the flexible wall under earthquake is derived. Based on the same assumption, Theodorakopoulos et al. [13] and Lanzoni et al. [14] presented the analytical solutions of dynamic response of cantilevered rigid wall and flexible wall in two-dimensional saturated site under earthquake. Based on the assumption of ignoring vertical displacement, Liu et al. [15, 16] obtained the analytical solution of dynamic response of flexible retaining wall under horizontal earthquake by semi-analytical method. Brandenberg et al. [17] gave the dynamic response analysis of rigid wall in non-uniform fill under earthquake. Ke et al. [18] proposed a simplified analytical solution of dynamic response of retaining wall considering the influence of soil shear stiffness. Based on the wave equation, Zhao et al. [19] studied the dynamic response of two-dimensional cantilever rigid wall under earthquake action, and gave a more rigorous analytical solution considering both vertical stress and vertical displacement.

The above analytical studies usually ignore the vertical stress or vertical displacement of the soil layer. Since the vibration equation of soil layer based on Biot theory is a coupling equation, it cannot be solved directly. Based on the two-dimensional soil layer vibration equation, this paper achieves the purpose of decoupling through differential transformation. Combined with the interaction conditions between the wall and the soil layer, a more rigorous analytical solution of the dynamic response of the cantilever flexible retaining wall is derived. The solution of this paper is reduced to rigidity and compared with the existing analytical solution of the rigid wall, which verifies the correctness of the analytical solution of this paper. At the same time, it is compared with the existing simplified analytical solution of the flexible retaining wall, and the difference between the simplified solutions and their application scope are pointed out.

2. Methodology

2.1. System considered

The system considered is shown in Fig. 1. The flexible retaining wall is embedded in the rigid foundation. The bottom of the wall is rigidly connected with the foundation. The upper surface of the soil layer is free, and the lower surface is full bound; The flexible retaining wall is homogeneous and elastic material, and the soil is homogeneous and isotropic semi-infinite linear body; Between the wall and soil fully bond; The wall and the bottom of the soil layer are subjected to a simple harmonic excitation of constant magnitude and the material damping is constant hysteretic damping. The wall height and soil thickness are H, the wall density is ρ_w, the elastic modulus of the wall is E_w, and the wall thickness is t_w. The relative flexibility coefficient d_w proposed by Veletsos and Younan [11] is defined as follows:

$$d_w = \frac{GH^3}{D_w} = 12(1-v_w^2)\frac{G}{E_w}\left(\frac{H}{t_w}\right) \tag{2.1}$$

where G is the soil shear modulus; D_w is the bending stiffness of the unit length wall; v_w is the poisson' s ratio of the wall.

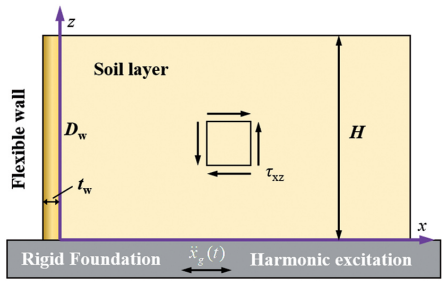

Fig. 1. Mechanical model of soil-flexible wall

The process of analytical solution is shown in Fig. 2.

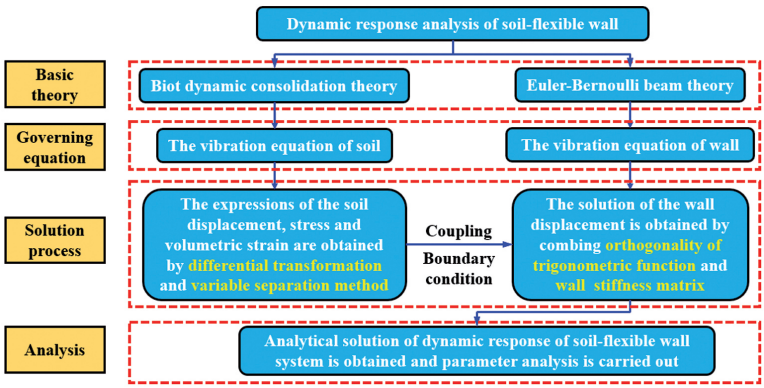

Fig. 2. The process of analytical solution

2.2. Governing equation

2.2.1. Governing equation of soil

According to Biot dynamic consolidation equation, the motion of the total system is expressed as [19]:

$$\frac{\partial \sigma_x}{\partial x} + \frac{\partial \tau_{xz}}{\partial z} = \rho \frac{\partial^2 u_x}{\partial t^2} + \rho \ddot{x}_g(t) \tag{2.2}$$

$$\frac{\partial \sigma_z}{\partial z} + \frac{\partial \tau_{xz}}{\partial x} = \rho \frac{\partial^2 u_z}{\partial t^2} \tag{2.3}$$

where σ_x, τ_{xz} and σ_z and are the horizontal normal stress, shear stress and vertical normal stress of the soil layer respectively; and u_x are u_z the x directional and z directional displacement of soil layer relative to rigid foundation respectively; ρ is the mass density of the soil; t is the time; $\ddot{x}_g(t)$ is the simple harmonic vibration acceleration. The signs of stress and displacement are positive along the positive direction of the coordinate axis and negative along the negative direction of the coordinate axis according to the elastic mechanics.

2.2.2. Governing equation of wall

The Euler–Bernoulli beam theory [20] is used to simulate the wall. The bending stiffness of the wall is $E_w I_w$, E_w is the elastic modulus of the wall, I_w is the section moment of inertia per unit length of the wall. Considering the horizontal force balance of the wall, the vibration equation of the wall is:

$$m \frac{\partial^2 u_w(z,t)}{\partial t^2} + E_w I_w \frac{\partial^4 u_w(z,t)}{\partial z^4} = \sigma_w(z,t) + m \ddot{x}_g(t) \tag{2.4}$$

where $u_w(z,t)$ is the horizontal displacement of the wall relative to the rigid foundation; $\sigma_w(z,t)$ is the soil pressure on the wall; m is the mass per unit length of the wall.

For the two-dimensional plane strain element, the relationship between stress and displacement is expressed as [19]:

$$\sigma_x = \lambda^* \theta + 2G^* \frac{\partial u_x}{\partial x} \tag{2.5a}$$

$$\tau_{xz} = G^* \left(\frac{\partial u_x}{\partial z} + \frac{\partial u_z}{\partial x} \right) \tag{2.5b}$$

$$\sigma_z = \lambda^* \theta + 2G^* \frac{\partial u_z}{\partial z} \tag{2.5c}$$

where G^* and λ^* is the complex Lame constant, $G^* = G(1 + i\delta)$, $\lambda^* = 2\nu G^*/(1 - 2\nu)$. δ is the soil material damping factor; ν is the soil Poisson's ratio, e is the soil volumetric strain, $e = \partial u_x/\partial x + \partial u_z/\partial z$.

2.3. Boundary conditions

1. The free surface shear stress is zero.

$$\tau_{xz}|_{z=H} = 0 \tag{2.6}$$

2. The displacement of relative rigid foundation at infinity is finite.

$$u_x|_{x\to\infty} \to \text{finite value}, \qquad u_z|_{x\to\infty} \to \text{finite value} \tag{2.7}$$

3. The bottom is in full bond with the rigid foundation, and the contact surface has no slip and detachment.

$$u_x|_{z=0} = 0, \qquad u_z|_{z=0} = 0 \tag{2.8}$$

4. The interface between soil and wall is full bond, it means that the contact interface has no slip and separation.

$$u_x|_{x=0} = u_w(z), \qquad u_z|_{x=0} = 0 \tag{2.9}$$

5. The bottom of the wall does not produce displacement and rotation relative to the rigid foundation.

$$u_w(z)|_{z=0} = 0, \qquad \left.\frac{du_w(z)}{dz}\right|_{z=0} = 0 \tag{2.10}$$

6. The wall top bending moment, shear force is zero.

$$\left.\frac{d^2u_w(z)}{dz^2}\right|_{z=H} = 0, \qquad \left.\frac{d^3u_w(z)}{dz^3}\right|_{z=H} = 0 \tag{2.11}$$

3. Solution of the equation

3.1. Solution of the governing equation of soil

For harmonic vibration, harmonic vibration acceleration, soil horizontal relative displacement, soil vertical relative displacement, soil volume strain, soil horizontal normal stress, soil horizontal shear stress and soil vertical normal stress can be written as follows:

$$\begin{gathered}\ddot{x}_g(t) = \ddot{X}_g e^{i\omega t}; \quad u_x = u_x(x,z)e^{i\omega t}; \quad u_z = u_z(x,z)e^{i\omega t}; \quad e = e(x,z)e^{i\omega t};\\ \sigma_x = \sigma_x(x,z)e^{i\omega t}; \quad \tau_{xz} = \tau_{xz}(x,z)e^{i\omega t}; \quad sigma_z = \sigma_z(x,z)e^{i\omega t}\end{gathered} \tag{3.1}$$

where $\ddot{X}_g$ is the amplitude of the input harmonic vibration acceleration; $u_x(x,z)$ is the horizontal displacement amplitude of the soil layer relative to the rigid foundation; $u_z(x,z)$ is the vertical displacement amplitude of the soil layer relative to the rigid foundation; e is the volumetric strain of soil. $\sigma_x(x,z)$ is the horizontal normal stress amplitude of the soil layer; $\tau_x(x,z)$ is the soil shear stress amplitude; $\sigma_z(x,z)$ is the vertical normal stress amplitude of the soil layer.

Because the whole system is a steady-state harmonic vibration with a circular frequency, the partial derivatives of both sides of Eq. 2.2 are solved, and the partial derivatives of both sides of Eq. 2.3 are solved, and then the two equations after operation are added.

$$(\lambda^* + G^*)\nabla^2 e + \rho\omega^2 e = 0 \tag{3.2}$$

where ∇^2 is the Laplace operator, denote as $\nabla^2 = \partial^2/\partial x^2 + \partial^2/\partial z^2$.

The equation is solved by the separation of variables method. Suppose that $e = U(x)W(z)e^{i\omega t}$, Eq. 3.2 can be rewritten as:

$$\frac{1}{U(x)}\frac{d^2U(x)}{\mathrm{dx}^2} + \frac{1}{W(z)}\frac{\mathrm{d}^2\mathrm{W(z)}}{\mathrm{dz}^2} + \beta_1^2 = 0 \tag{3.3}$$

where $\beta_1^2 = \dfrac{\rho\omega^2}{\lambda^* + 2G^*}$.

According to the theory of differential equations, the solution of Eq. 3.2 can be written as:

$$U(x) = A_1 e^{g_1 x} + B_1 e^{-g_1 x} \tag{3.4}$$

$$W(z) = C_1 \sin(g_2 z) + D_1 \cos(g_2 z) \tag{3.5}$$

where A_1, B_1, C_1, D_1, g_1 and g_2 are undetermined constants; $g_2^2 - g_1^2 = \beta_1^2$.

Therefore:

$$e = e^{\mathrm{i}\omega\mathrm{t}}(A_1 e^{g_1 x} + B_1 e^{-g_1 x})[C_1 \sin(g_2 z) + D_1 \cos(g_2 z)] \tag{3.6}$$

According to the boundary condition (2.7), when $x \to \infty$, the dynamic response of soil layer is finite, so it will not increase infinitely. Reintegrating the constant coefficient term of Eq. (3.6), it can be simplified as:

$$e = e^{i\omega t} e^{-g_1 x}[A_2 \sin(g_2 z) + B_2 \cos(g_2 z)] \tag{3.7}$$

where A_2 and B_2 are undetermined constants.

Therefore, the solution of soil volumetric strain containing undetermined constants has been obtained, and then it is substituted back to the soil motion equation to solve the soil displacement.

Eqs. (2.2) and (2.3) are rewritten as:

$$G^*\nabla^2 u_z + \rho\omega^2 u_z = -(\lambda^* + G^*)\frac{\partial\theta}{\partial z} + \rho\ddot{x}_g(t) \tag{3.8}$$

$$G^*\nabla^2 u_z + \rho\omega^2 u_z = -(\lambda^* + G^*)\frac{\partial\theta}{\partial z} \tag{3.9}$$

Observing Eqs. (3.8) and (3.9), it can be seen that the two equations are non-homogeneous equations about x and z, respectively. The solution of the equation can be obtained by solving the general solution of the corresponding homogeneous equation and adding the particular solution.

The homogeneous equation corresponding to Eq. (3.8) is as follows:

$$G^*\nabla^2 u_x^h + \rho\omega^2 u_x^h = 0 \tag{3.10}$$

where u_x^h is the general solution.

Assume that $\beta_2^2 = \dfrac{\rho\omega^2}{G^*}$, we can obtained:

$$u_x^h = e^{i\omega t}(A_3 e^{g_3 x} + B_3 e^{-g_3 x})[C_3 \sin(g_4 z) + D_3 \cos(g_4 z)] \tag{3.11}$$

where A_3,B_3, C_3, D_3, g_3, g_4 and are undetermined constants; $g_4^2 - g_3^2 = \beta_2^2$.

Combined with the boundary condition (2.2), the constant coefficient term in the integrated Eq. (2.2) can be simplified to:

$$u_x^h = e^{i\omega t} e^{-g_3 x}[A_4 \sin(g_4 z) + B_4 \cos(g_4 z)] \tag{3.12}$$

where A_4 and B_4 are undetermined constants.

Observing the inhomogeneous Eq. (3.8), its particular solution can be set as

$$u_x^p = e^{i\omega t}\{e^{-g_1 x}[A_5 \sin(g_2 z) + B_5 \cos(g_2 z)] + C_4\} \tag{3.13}$$

where A_5, B_5 and C_4 are undetermined constants.

$$\begin{aligned} u_x = e^{i\omega t}\big\{ & e^{-g_3 x}\,[A_4 \sin(g_4 z) + B_4 \cos(g_4 z)] \\ & + e^{-g_1 x}\,[A_5 \sin(g_2 z) + B_5 \cos(g_2 z)] + C_4\big\} \end{aligned} \tag{3.14}$$

Similarly, the solution of Eq. (3.9) is expressed as:

$$u_z = e^{i\omega t}\{e^{-g_3 x}[A_6 \sin(g_4 z) + B_6 \cos(g_4 z)] + e^{-g_1 x}[A_7 \sin(g_2 z) + B_7 \cos(g_2 z)]\} \tag{3.15}$$

where A_6, A_7, B_6 and B_7 are undetermined constants.

Since the soil layer is dominated by horizontal vibration, combined with the boundary conditions (2.6) and (2.8), the eigenvalue of the vibration equation can be taken as:

$$g_4 = g_2 = g_n = \frac{n\pi}{2H}, n = 1, 3, 5\ldots \tag{3.16}$$

Combined with superposition principle, the solution of soil horizontal displacement, soil vertical displacement and soil bulk modulus amplitude can be written in the form of the following series sum:

$$u_x(x, z) = \sum_{n=1,3}^{\infty} (E_1 e^{-g_3 x} + E_2 e^{-g_1 x} + E_3) \sin(g_n z) \tag{3.17}$$

$$u_z(x, z) = \sum_{n=1,3}^{\infty} (E_4 e^{-g_3 x} + E_5 e^{-g_1 x}) \cos(g_n z) \tag{3.18}$$

$$e(x, z) = \sum_{n=1,3}^{\infty} A_2 e^{-g_1 x} \sin(g_n z) \tag{3.19}$$

where E_1, E_2, E_3, E_4 and E_5 are all undetermined constants.

Substituting Eqs. (3.17), (3.18) and (3.19) to Eqs. (3.8) and (3.9), combine with $e = \frac{\partial u_x}{\partial x} + \frac{\partial u_z}{\partial z}$, and extend $\ddot{X}_g$ to the sum of series:

$$\ddot{X}_g = \sum_{n=1,3}^{\infty} \frac{4}{n\pi} \ddot{X}_g \sin(g_n z) \tag{3.20}$$

Thus

$$u_x(x,z) = \sum_{n=1,3}^{\infty} \left(A_4 e^{-g_3 x} + \lambda_1 A_2 e^{-g_1 x} + \frac{\rho \ddot{X}_g \frac{4}{n\pi}}{\rho\omega^2 - G^* \left(\frac{n\pi}{2H}\right)^2} \right) \sin(g_n z) \tag{3.21}$$

$$u_z(x,z) = \sum_{n=1,3}^{\infty} \left(-\frac{g_3}{g_4} A_4 e^{-g_3 x} - \lambda_2 A_2 e^{-g_1 x} \right) \cos(g_n z) \tag{3.22}$$

$$e(x,z) = \sum_{n=1,3}^{\infty} A_2 e^{-g_1 x} \sin(g_n z) \tag{3.23}$$

Substituting Eqs. (3.21) and (3.23) into Eq. (2.5a), the horizontal normal stress amplitude of soil layer is

$$\sigma_x(x,z) = \sum_{n=1,3}^{\infty} \left[(\lambda^* - 2G^* g_1 \lambda_1) A_2 e^{-g_1 x} - 2G^* g_3 A_4 e^{-g_3 x} \right] \sin(g_n z) \tag{3.24}$$

In order to solve the dynamic response of flexible wall, the boundary condition $(2.4)_2$ is substituted into Eq. (3.22):

$$\frac{g_3}{g_4} A_4 - \lambda_2 A_2 = 0 \tag{3.25}$$

Assume that $A_n = \frac{g_3}{g_4} A_4$, we can obtain $A_4 = \frac{g_4}{g_3} A_n$, $A_2 = -\frac{1}{\lambda_2} A_n$ where A_n is the undetermined constant.

Substituting Eq. (3.25) into Eqs. (3.21) and (3.24) and sorting, the amplitude of earth pressure on the wall and the displacement amplitude of the wall can be obtained:

$$\sigma_x(0,z) = \sigma_w(z) = \sum_{n=1,3}^{\infty} F_{1n} A_n \sin(g_n z) \tag{3.26}$$

$$u_x(0,z) = u_w(z) = \sum_{n=1,3}^{\infty} (F_{2n} A_n + F_{3n}) \sin(g_n z) \tag{3.27}$$

where $F_{1n} = \frac{2G^* g_1 \lambda_1 - \lambda^* - 2\lambda_2 G^* g_4}{\lambda_2}$, $F_{2n} = \frac{g_4}{g_3} - \frac{\lambda_1}{\lambda_2}$, $F_{3n} = \frac{\rho \ddot{X}_g \frac{4}{n\pi}}{\rho\omega^2 - G^* \left(\frac{n\pi}{2H}\right)^2}$.

Therefore, the undetermined constant is only A_n and it can be determined by the coupling relationship with the wall.

3.2. Solution of the governing equation of wall

Substitute Eqs. (3.1), (3.26) and (3.27) into Eq. (2.4):

$$\frac{d^4 u_w(z)}{\partial z^4} - \beta^4 u_w(z) = \frac{1}{E_w I_w} \sum_{n=1,3}^{\infty} \left(F_{1n} A_n + \frac{4m\ddot{X}_g}{n\pi} \right) \sin(g_n z) \tag{3.28}$$

where $\beta^4 = \dfrac{m\omega^2}{E_w I_w}$.

The general solution of the homogeneous equation corresponding to Eq. (3.28) is expressed as:

$$u_w^h(z) = B_1 \sin(\beta z) + B_2 \cos(\beta z) + B_3 \sinh(\beta z) + B_4 \cosh(\beta z) \tag{3.29}$$

where B_1, B_2, B_3 and B_4 are undetermined constants.

Assume the particular solution of Eq. (3.28) that:

$$u_w^p(z) = \sum_{n=1,3}^{\infty} B_n \sin(g_n z) \tag{3.30}$$

Substituting the particular solution back to Eq. (3.23), we get:

$$B_n = \frac{F_{1n} A_n + \dfrac{4m\ddot{X}_g}{n\pi}}{E_w I_w (g_n^4 - \beta^4)} \tag{3.31}$$

The solution of the system of Eq. (3.28) is expressed as:

$$\begin{aligned} u_w(z) = {} & B_1 \sin(\beta z) + B_2 \cos(\beta z) + B_3 \sinh(\beta z) + B_4 \cosh(\beta z) \\ & + \sum_{n=1,3}^{\infty} \frac{F_{1n} A_n + \dfrac{4m\ddot{X}_g}{n\pi}}{E_w I_w \left(g_n^4 - \beta^4\right)} \sin(g_n z) \end{aligned} \tag{3.32}$$

By the boundary condition $(2.9)_1$, there is no slip between the contact surface of the wall and the soil, there are:

$$\begin{aligned} & B_1 \sin(\beta z) + B_2 \cos(\beta z) + B_3 \sinh(\beta z) \\ & + B_4 \cosh(\beta z) + \sum_{n=1,3}^{\infty} \frac{F_{1n} A_n + \dfrac{4m\ddot{X}_g}{n\pi}}{E_w I_w \left(g_n^4 - \beta^4\right)} \sin(g_n z) \\ & = \sum_{n=1,3}^{\infty} (F_{2n} A_n + F_{3n}) \sin(g_n z) \end{aligned} \tag{3.33}$$

Using the orthogonality of the sine function on the interval, the two ends of the equal sign of Eq. (3.33) are multiplied, and then integrated on the interval to obtain:

$$A_n = \frac{2N_n E_w I_w (g_n^4 - \beta^4) + \dfrac{4mH\ddot{X}_g}{n\pi} - HF_{3n} E_w I_w (g_n^4 - \beta^4)}{HF_{2n} E_w I_w (g_n^4 - \beta^4) - HF_{1n}} \tag{3.34}$$

where

$$N_n = N_1 B_1 + N_2 B_2 + N_3 B_3 + N_4 B_4; \qquad N_1 = \frac{-\beta \cos(\beta H)(-1)^{(n-1)/2}}{\beta^2 - g_n^2};$$

$$N_2 = \frac{\beta \sin(\beta H)(-1)^{(n-1)/2} - g_n}{\beta^2 - g_n^2}; \qquad N_3 = \frac{-\beta \cosh(\beta H)(-1)^{(n-1)/2}}{\beta^2 + g_n^2};$$

$$N_4 = \frac{-\beta \sinh(\beta H)(-1)^{(n-1)/2} + g_n}{\beta^2 + g_n^2}$$

The solution of Eq. (3.28) is expressed as:

$$u_w(z) = B_1 f_1(z) + B_2 f_2(z) + B_3 f_3(z) + B_4 f_4(z) + f_p(z) \tag{3.35}$$

where

$$f_1(z) = \sin(\beta z) + \sum_{n=1,3}^{\infty} \zeta N_1 \sin(g_n z); \qquad f_2(z) = \sin(\beta z) + \sum_{n=1,3}^{\infty} \zeta N_2 \sin(g_n z);$$

$$f_3(z) = \sin(\beta z) + \sum_{n=1,3}^{\infty} \zeta N_3 \sin(g_n z); \qquad f_4(z) = \sin(\beta z) + \sum_{n=1,3}^{\infty} \zeta N_4 \sin(g_n z);$$

$$f_p(z) = \sum_{n=1,3}^{\infty} F_{4n} \sin(g_n z)$$

In which

$$F_{4n} = \frac{\dfrac{4mF_{1n}\ddot{X}_g}{n\pi E_w I_w (g_n^4 - \beta^4)} - F_{1n}F_{3n}}{F_{2n} E_w I_w (g_n^4 - \beta^4) - F_{1n}} + \frac{4m\ddot{X}_g}{n\pi E_w I_w (g_n^4 - \beta^4)};$$

$$\zeta = \frac{2F_{1n}}{HF_{2n} E_w I_w (g_n^4 - \beta^4) - HF_{1n}}$$

Therefore, combined with boundary conditions (2.10) and (2.11), the following matrix can be obtained:

$$\begin{bmatrix} f_1(z) & f_2(z) & f_3(z) & f_4(z) \\ f_1'(z) & f_2'(z) & f_3'(z) & f_4'(z) \\ f_1''(z) & f_2''(z) & f_3''(z) & f_4''(z) \\ f_1'''(z) & f_2'''(z) & f_3'''(z) & f_4'''(z) \end{bmatrix} \begin{Bmatrix} B_1 \\ B_2 \\ B_3 \\ B_4 \end{Bmatrix} + \begin{Bmatrix} f_p(z) \\ f_p'(z) \\ f_p''(z) \\ f_p'''(z) \end{Bmatrix} = \begin{Bmatrix} 0 \\ 0 \\ 0 \\ 0 \end{Bmatrix} \tag{3.36}$$

where the superscript represents the partial derivative.

By calculating the above matrix, all unknown constants (B_1, B_2, B_3 and B_4) can be determined.

3.3. Soil normal stress and shear stress

Substituting Eq. (3.26) into Eq. (3.34), the horizontal normal stress amplitude of soil layer is

$$\sigma_x(x,z) = \sum_{n=1,3}^{\infty} \left[\frac{(2G^* g_1 \lambda_1 - \lambda^*)}{\lambda_2} A_n e^{-g_1 x} - 2G^* g_4 A_n e^{-g_3 x} \right] \sin \frac{n\pi}{2H} z \tag{3.37}$$

Substituting Eqs. (3.21), (3.22) and (3.26) into Eq. (2.5b), the shear stress amplitude of the soil layer is written that:

$$\tau_{xz}(x,z) = \sum_{n=1,3}^{\infty} G^* \left[\frac{n\pi}{2H} \left(\frac{g_4}{g_3} A_n e^{-g_3 x} - \frac{\lambda_1}{\lambda_2} A_n e^{-g_1 x} + \frac{\rho \ddot{X}_g \frac{4}{n\pi}}{\rho\omega^2 - G^* \left(\frac{n\pi}{2H} \right)^2} \right) + g_3 A_n e^{-g_3 x} - g_1 A_n e^{-g_1 x} \right] \cos \frac{n\pi}{2H} z \tag{3.38}$$

3.4. Wall bottom bending moment and shear force

The expression of the shear force amplitude and the corresponding bending moment amplitude per unit length of the wall bottom can be determined by integrating the expression (3.37) of the wall-side earth pressure amplitude:

$$Q_b = \sum_{n=1,3}^{\infty} \frac{2H}{n\pi} \left(\frac{2G^* g_1 \lambda_1 - \lambda^*}{\lambda_2} A_n - 2G^* g_4 A_n \right) \tag{3.39}$$

$$M_b = \sum_{n=1,3}^{\infty} (-1)^{(n-1)/2} \frac{4H^2}{n^2\pi^2} \left(\frac{2G^* g_1 \lambda_1 - \lambda^*}{\lambda_2} A_n - 2G^* g_4 A_n \right) \tag{3.40}$$

4. Results and analysis

In the following analysis, $\omega_1 = \pi v_s/(2H)$ is the natural frequency of the soil layer, where $v_s = \sqrt{G/\rho}$. For the convenience of comparison, except for special instructions, the parameter values in this paper refer to Reference [11], Poisson's ratio v is 0.3, material damping is 0.1, soil density is 2300 kg/m^3, soil shear modulus is 3×10^7 Pa, base acceleration amplitude is 3 m/s^2, wall height is 5 m, the Poisson's ratio of wall is 0.2, the thickness of wall is 0.125 m.

4.1. Comparative validation of results

In order to verify the rationality of the solution in this paper, the dynamic response analysis of the flexible wall in this paper is degenerated into the dynamic response analysis of the rigid wall. And compared with the rigid wall analytical solution proposed by Zhao et

al. [19], as shown in Fig. 3. It can be seen from Fig. 3 that when the solution of this present degenerates into the solution of rigid wall, which is completely consistent with the solution of the earth pressure on the top of rigid wall proposed by Zhao et al., which verifies the accuracy of the calculation result of the dynamic earth pressure on the top of flexible wall.

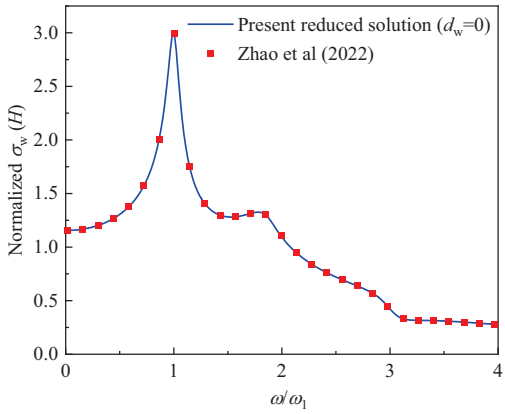

Fig. 3. Comparison and verification of the inverse present solution with the solution proposed by Zhao et al. (2022)

The present solution is compared with the solution that ignoring vertical stress proposed by Veletsos et al. [11], as shown in Fig. 4. When the excitation frequency is low, ignoring the vertical stress solution is slightly larger than the present solution. The friction between the soil walls is considered in the process of solving, and the relative motion between the soil walls is allowed in the model ignoring the vertical stress solution. This difference makes the dynamic response that assume no vertical stress solution develop in soil medium slightly larger than that of present solution. When the excitation frequency is high, the solution

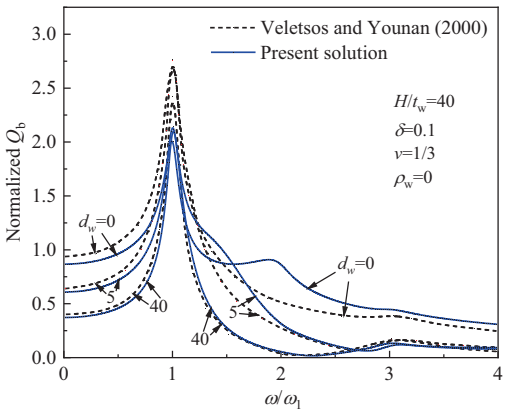

Fig. 4. Comparison and verification of the present solutions with the solution proposed by Veletsos and Younan (2000)

proposed by Veletsos et al is slightly smaller than the present solution. The reason for this phenomenon is that the solution proposed by Veletsos et al that ignore the vertical stress and the vibration superposition effect caused by it. In addition, it can be seen from Fig. 4 that when the relative flexibility coefficient is large, the two solutions are very close except for the first-order resonance point, indicating that the dynamic response of the flexible wall can be approximately considered by ignoring the vertical stress solution when the relative flexibility coefficient is large.

The variation of wall top earth pressure with Poisson's ratio is compared with the solution that ignoring vertical stress and the solution that ignoring vertical displacement, as shown in Fig. 5.

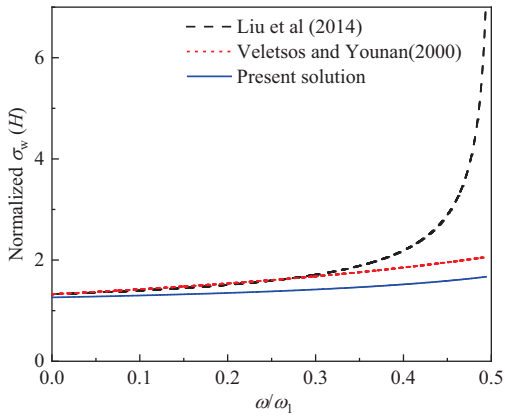

Fig. 5. Variation of earth pressure on top of wall with Poisson's ratio of soil

Take frequency, relative flexibility coefficient. It can be seen from Fig. 5 that the solution that ignoring vertical displacement and the solution that ignoring vertical stress are basically consistent and close to the present solution. At that time, the solution that ignoring vertical displacement increases rapidly. When it is close to 0.5, this solution has lost its meaning.

4.2. Size and distribution of earth pressure on the wall

Figure 6a shows the distribution of earth pressure along the height of flexible wall under different excitation frequencies. As can be seen from the figure, when $\omega/\omega_1 < 1$, the wall earth pressure increases with the excitation frequency increases; when $\omega/\omega_1 = 1$, the earth pressure on the wall takes the maximum value at any position; when $\omega/\omega_1 > 1$, the amplitude of earth pressure on the wall decreases with the increase of frequency. It can be seen from Fig. 6b that when the excitation frequency is high, namely $\omega/\omega_1 = 3$, the real and imaginary parts of the earth pressure on the wall are large, indicating that the influence of the damping part corresponding to the imaginary part cannot be ignored when the excitation frequency is high.

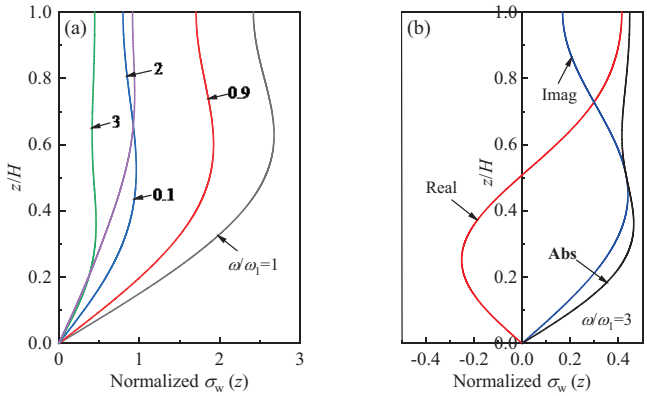

Fig. 6. Distribution of wall pressures and displacements along the wall height for different frequencies: (a) different frequencies; (b) $\omega/\omega_1 = 3$

4.3. Horizontal distribution of soil stress and displacement

Figure 7 shows the horizontal distribution of stress and displacement of soil-flexible wall system under different excitation frequencies. The results show that:

1. The distribution law of horizontal normal stress of soil layer: when ω/ω_1 is 1 or less, the maximum value of horizontal normal stress of soil layer appears near the wall, and only a turning point occurs near the wall. After the turning point, it decreases monotonously with the increase of distance from the wall, and tends to 0 in the far field. When ω/ω_1 is 2 or greater, with the increase of the distance from the wall, the horizontal normal stress of the soil layer shows a wavy change with the increase of the distance from the wall and gradually decreases, and tends to 0 in the far field.
2. The distribution law of horizontal displacement of soil layer: when ω/ω_1 is 1 or smaller, the horizontal displacement of soil layer increases monotonically from the wall to the far field, and the far field tends to a constant. When ω/ω_1 is 2 or greater, the horizontal displacement of the soil layer shows a wavy change with the increase of the distance

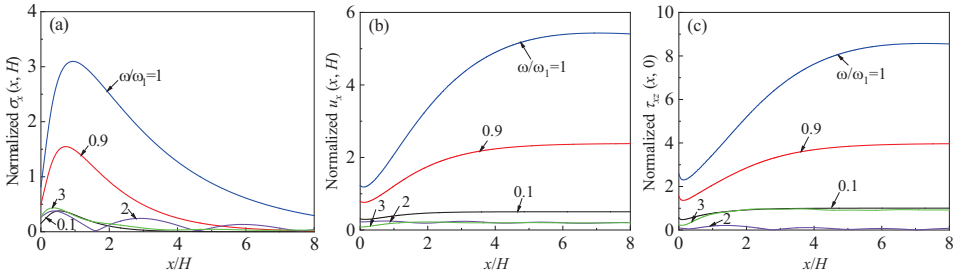

Fig. 7. Variation of horizontal normal stress of the top layer with excitation frequencies along the horizontal axis

from the wall. In the far field, it also tends to a smaller constant, and the radiation damping effect is obvious.

3. Distribution law of soil shear stress: when the excitation frequency is low, that is, 0.1 or greater, the minimum value of soil shear stress amplitude appears near the wall, and then increases monotonically with the distance from the wall. When ω/ω_1 is 2 or more, the soil shear stress changes with the distance from the wall.

The above rules show that when the excitation frequency is low, the amplitude of the earth pressure on the wall and the displacement of the wall are mainly controlled by the soil near the wall. When the excitation frequency is high, the far-field soil has a non-negligible influence on the amplitude of the earth pressure on the wall and the displacement of the wall.

4.4. Bottom shear and bending moment

Figure 8 show the distribution of shear force and bending moment at the bottom of unit length wall with different frequencies. It can be seen from Fig. 8 that with the increase of the relative flexibility coefficient of the wall, the shear force and bending moment at the bottom of the wall generally decrease. This may be because the flexible wall can reduce the shear force and bending moment at the bottom of the wall by adjusting its shape. However, at the first order resonance frequency, when the frequency ratio is 1, the amplitude of the base shear force increases slightly with the increase of the relative elastic coefficient of the wall. The shear force at the bottom of the wall decreases with the increase of the relative flexibility coefficient of the wall, but the range is not large. For the bending moment at the bottom of the wall, the reduction at the resonance frequency is greater than the reduction of the shear force. It can be seen from the figure that when the relative flexibility coefficient of the wall is 5 or smaller, the shear force and bending moment amplitude at the bottom of the wall are greatly affected by the relative flexibility coefficient of the wall, especially when it is 2 or larger.

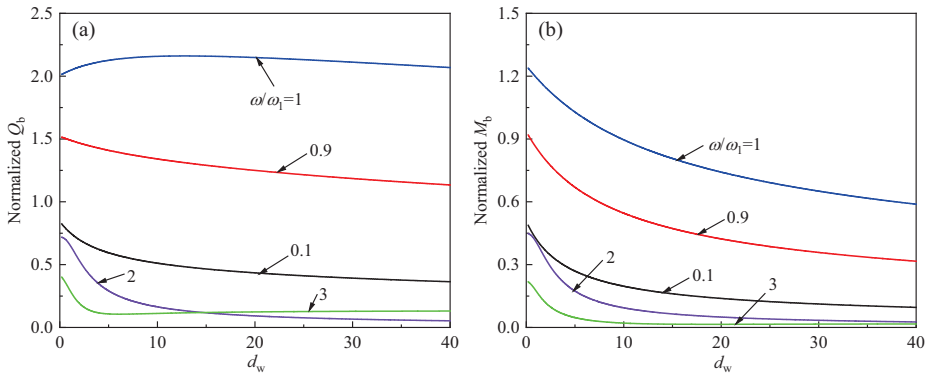

Fig. 8. Variation of shear force at the bottom of the wall with relative elasticity

Figure 9 give the magnification factors of the shear force and bending moment at the bottom of the wall under dynamic excitation relative to static excitation.

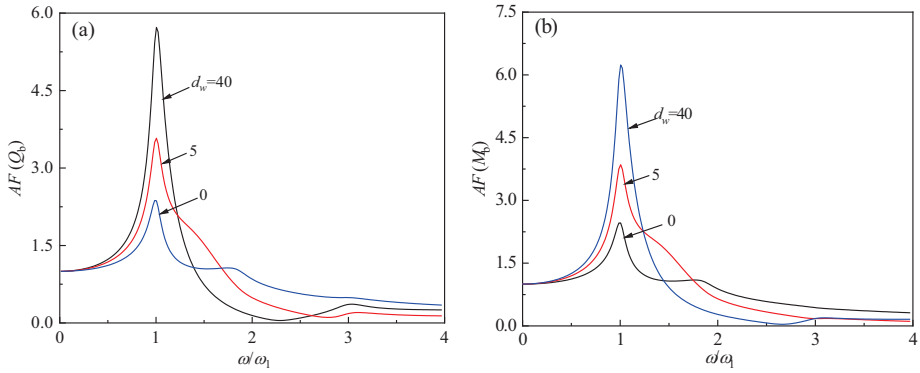

Fig. 9. The dynamic amplification factor of the wall bottom shear force

It can be seen that whether it is the shear force or the bending moment at the bottom of the wall, the peak value of the amplification factor appears at the natural frequency of the soil layer, and the amplification factor here is much larger than that at other excitation frequencies, especially at high excitation frequencies, indicating that the basic vibration mode is the main contributor to the dynamic response of the wall and plays a controlling role. At that time, the dynamic amplification factor of shear force and bending moment at the bottom of the wall decreased rapidly to less than 1, indicating that the radiation damping effect was obvious and the radiation energy dissipation of the wave was more. In addition, it can be seen from the Fig. 9 that the peak value of the amplification factor is quite sensitive to the relative flexibility coefficient of the wall, and the larger, the greater the peak value of the amplification factor. Therefore, in the seismic design of underground engineering, for walls with low stiffness, special attention should be paid to the shear force and bending moment at the bottom of the wall under the first resonance frequency.

The convergence characteristics of the shear force and bending moment at the bottom of the flexible wall are given in Fig. 10. As the calculation results converge when the order of modes is greater than 50, the first 50 modes are approximately considered as all modes. It can be seen from Fig. 10 that if only the first-order vibration mode is considered, there is

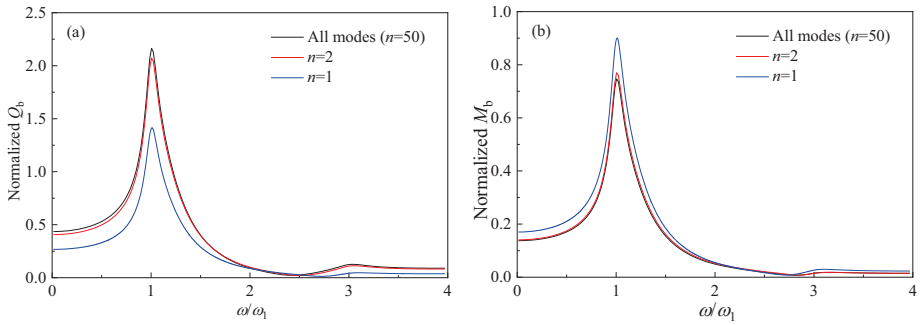

Fig. 10. The change of wall shear force with frequency considering different modal numbers

still a large error in the accurate value of the shear force at the bottom of the wall compared with the bending moment, especially at low excitation frequencies. If the first two vibration modes are considered, the solution at this time is very close to the exact value, and the error is negligible.

5. Conclusions

Based on Biot theory and Euler–Bernoulli beam theory, a more rigorous analytical solution for the dynamic response of vertical flexible retaining wall in homogeneous soil is derived. The following main conclusions can be obtained through analysis:

1. The solution of this paper is degenerated and compared with the existing solution. It shows that the degenerate solution is in good agreement with the existing solution, which proves that the solution of this paper is reasonable. When the Poisson's ratio of soil is less than 0.3, ignoring the vertical displacement and vertical stress are close to the more rigorous solution in this paper. When the Poisson's ratio of soil is greater than 0.3, the solution of ignoring vertical displacement increases rapidly. When the Poisson's ratio of the soil tends to 0.5, ignoring the vertical displacement solution cannot be used as a reference.
2. When the excitation frequency is low, the earth pressure on the wall and the displacement amplitude of the wall are mainly controlled by the soil near the wall. When the excitation frequency is high, the influence of the far-field soil on the earth pressure and the displacement of the wall gradually increases, and its influence cannot be ignored.
3. Wall displacement, wall soil pressure, wall bottom internal force and its amplification coefficient are highly correlated with the relative flexibility coefficient of the wall. With the increase of the relative flexibility coefficient of the wall, the wall displacement and the amplification coefficient of the internal force of the wall bottom increase, the earth pressure on the wall decreases, and the shear force of the wall bottom decreases with the increase of the relative flexibility coefficient of the wall except the first order resonance frequency.
4. The shear force and bending moment at the bottom of the wall can be approximately expressed by the first two vibration modes.

At present, the research on the dynamic response of retaining walls under earthquake mainly focuses on analytical research, and the main contribution of this study is to obtain a more rigorous analytical solution. However, the actual seismic waves are not simple harmonics, so the research in this study cannot be directly used in engineering practice. In the future, a variety of seismic waves will be considered as input waves to carry out a more intuitive study on dynamic response of retaining wall which can directly reflect seismic wave.

Acknowledgements

The study was supported by the National Natural Science Foundation of China under Grant No. 51978671. The authors are grateful for the great support awarded.

References

[1] J. Mousavi and S. Tariverdilo, "Tuning mass of internal flexible wall to reduce seismic demand on exterior walls of liquid storage tanks", *Engineering Structures*, vol. 101, no. 15, pp. 279–289, 2015, doi: 10.1016/j.engstruct.2015.07.011.

[2] O.L. Ertugrul and A.C. Trandafir, "Seismic earth pressures on flexible cantilever retaining walls with deformable inclusions", *Journal of Rock Mechanics and Geotechnical Engineering*, vol. 6, no. 5, pp. 417–427, 2014, doi: 10.1016/j.jrmge.2014.07.004.

[3] J.S. Xu, X.L. Du, and X.L. Yang, "Stability analysis of 3D geosynthetic-reinforced earth structures composed of nonhomogeneous cohesive backfills", *Soil Dynamics and Earthquake Engineering*, vol. 126, art. no. 105768, 2019, doi: 10.1016/j.soildyn.2019.105768.

[4] M. Grodecki, "Numerical modelling of gabion retaining wall under loading and unloading", *Archives of Civil Engineering*, vol. 67, no. 2, pp. 155–164, 2021, doi: 10.24425/ace.2021.137160.

[5] A. Bahrami and M. Yavari, "Analysis of composite shear walls with a gap between reinforced concrete wall and steel frame", *Archives of Civil Engineering*, vol. 66, no. 1, pp. 41–53, 2020, doi: 10.24425/ace.2020.131773.

[6] R.B. Han, C.S. Xu, Z.G. Xu, et al., "A boundary forced response displacement method for seismic analysis of symmetrical underground structures", *Engineering Mechanics*, vol. 38, no. 5, pp. 50–60, 2021, doi: 10.6052/ j.issn.1000-4750.2020.02.0075.

[7] J.B. Liu, D.Y. Wang, et al., "Theorectical derivation and consistency proof of the integral response deformation method", *China Civil Engineering Journal*, vol. 52, no. 8, pp. 18–23, 2019, doi: 10.15951/j.tmgcxb.2019.08.002.

[8] Z.D. Gao, M. Zhao, X.L. Du, and Z. Zhong, "A generalized response spectrum method for seismic response analysis of underground structure combined with viscous spring artificial boundary", *Soil Dynamics and Earthquake Engineering*, vol. 140, art. no. 106451, 2021, doi: 10.1016/j.soildyn.2020.106451.

[9] D. P. Qiu, J. Y. Chen, and Q. Xu, "Improved pushover analysis for underground large-scale frame structures based on structural dynamic responses", *Tunnelling and Underground Space Technology*, vol. 103, art. no. 103405, 2020, doi: 10.1016/j.tust.2020.103405.

[10] V.G. Kitsis, G.A. Athanasopoulos, and A. Athanasopoulos-Zekkos, "Earth retaining walls with backfill possessing cohesion-Numerical analyses of seismic behavior", *Soil Dynamics and Earthquake Engineering*, vol. 160, art. no. 107368, 2022, doi: 10.1016/j.soildyn.2022.107368.

[11] A.S. Veletsos and A.H. Younan, "Dynamic response of cantilever retaining walls", *Journal of Geotechnical and Geoenvironmental Engineering*, vol. 123, no. 2, pp. 161–172, 1997, doi: 10.1061/(ASCE)1090-0241(1997) 123:2(161).

[12] A.H. Younan and A.S. Veletsos, "Dynamic response of flexible retaining walls", *Earthquake Engineering and Structural Dynamics*, vol. 29, no. 12, pp. 1815–1844, 2000, doi: 10.1002/1096-9845(200012)29:12<1815::AID-EQE993>3.0.CO;2-Z.

[13] D.D. Theodorakopoulos, A.P. Chassiakos, and D.E. Beskos, "Dynamic pressures on rigid cantilever walls retaining poroelastic soil meida. Part ?: first method of solution", *Soil Dynamics and Earthquake Engineering*, vol. 21, no. 4, pp. 315–338, 2001, doi: 10.1016/S0267-7261(01)00009-4.

[14] L. Lanzoni, E. Radi, and A. Tralli, "On the seismic response of a flexible wall retaining a viscous poroelastic soil", *Soil Dynamics and Earthquake Engineering*, vol. 27, pp. 818–842, 2007, doi: 10.1016/j.soildyn.2007.01.009.

[15] Q.J. Liu, Y.X. Tian, and F.J. Deng, "Dynamic analysis of flexible cantilever wall retaining elastic soil by a modified Vlasov-Leontiev model", *Soil Dynamics and Earthquake Engineering*, vol. 63, pp. 217–225, 2014, doi: 10.1016/j.soildyn.2014.03.019.

[16] Q.J. Liu, "Modal analysis for kinematic response of flexible cantilever retaining wall", *Soils and Foundations*, vol. 56, no. 3, pp. 399–411, 2016, doi: 10.1016/j.sandf.2016.04.007.

[17] S.J. Brandenberg, G. Mylonakis, and J.P. Stewart, "Approximate solution for seismic earth pressure on rigid walls retaining in homogeneous elastic soil", *Soil Dynamics and Earthquake Engineering*, vol. 97, pp. 468–477, 2017, doi: 10.1016/j.soildyn.2017.03.028.

[18] W.H. Ke, W.J. Luo, T. Fang, et al., "A simple closed-form solution for kinematic responses of retaining wall incorporating the effects of shear stiffness of soils", *Soil Dynamics and Earthquake Engineering*, vol. 134, art. no. 106163, 2020, doi: 10.1016/j.soildyn.2020.106163.

[19] S. Zhao, J. Yu, X. Liu, et al., "Analytical study on dynamic response of cantilever underground rigid wall", *Rock and Soil Mechanics*, vol. 43, no. 1, pp. 152–159, 2022, doi: 10.16285/j.rsm.2021.0690.

[20] J. Yu, Y. He, L. Zhang, et al., "Dynamical characteristics of piles in liquefied soil under horizontal vibration", *Chinese Journal of Geotechnical Engineering*, vol. 39, no. 3, pp. 573–580, 2017, doi: 10.11779/CJGE 201703023.

Received: 2022-11-01, Revised: 2023-01-10